THE JOURNAL OF BIOLOGICAL CHEMISTRY VOL. 291, NO. 40, pp. 21184–21194, September 30, 2016

Characterization of a Novel D-Glycero-D-talo-oct-2-ulosonic acid-substituted Lipid A Moiety in the Lipopolysaccharide Produced by the Acetic Acid Bacterium *Acetobacter pasteurianus* NBRC 3283*

Received for publication, August 7, 2016 Published, JBC Papers in Press, August 18, 2016, DOI 10.1074/jbc.M116.751271

Masahito Hashimoto[‡1], Mami Ozono[‡], Maiko Furuyashiki[‡], Risako Baba[‡], Shuhei Hashiguchi[‡], Yasuo Suda[‡], Koichi Fukase[§], and Yukari Fujimoto[¶]

From the [‡]Department of Chemistry, Biotechnology, and Chemical Engineering, Kagoshima University, Kagoshima 890-0065, Japan, the [§]Department of Chemistry, Graduate School of Science, Osaka University, Osaka 560-0043, Japan, and the [¶]Faculty of Science and Technology, Keio University, Kanagawa 223-8522, Japan

Acetobacter pasteurianus **is an aerobic Gram-negative rod that is used in the fermentation process used to produce the traditional Japanese black rice vinegar kurozu. Previously, we found that a hydrophobic fraction derived from kurozu stimulates Toll-like receptors to produce cytokines. LPSs, particularly LPS from *A. pasteurianus*, are strong candidates for the immunostimulatory component of kurozu. The LPS of *A. pasteurianus* remains stable in acidic conditions during the 2 years of the abovementioned fermentation process. Thus, we hypothesized that its stability results from its structure. In this study, we isolated the LPS produced by *A. pasteurianus* NBRC 3283 bacterial cells and characterized the structure of its lipid A component. The lipid A moiety was obtained by standard weak acid hydrolysis of the LPS. However, the hydrolysis was incomplete because a certain proportion of the LPS contained acid-stable D-glycero-D-talo-oct-2-ulosonic acid (Ko) residues instead of the acid-labile 3-deoxy-D-manno-oct-2-ulosonic acid residues that are normally found in typical LPS. Even so, we obtained a Ko-substituted lipid A with a novel sugar backbone, α-Man(1–4)[α-Ko(2–6)]β-GlcN3N(1–6)α-GlcN(1–1)α-GlcA. Its reducing end GlcN(1-1)GlcA bond was also found to be quite acid-stable. Six fatty acids were attached to the backbone. Both the whole LPS and the lipid A moiety induced TNF-α production in murine cells via Toll-like receptor 4, although their activity was weaker than those of *Escherichia coli* LPS and lipid A. These results suggest that the structurally atypical *A. pasteurianus* lipid A found in this study remains stable and, hence, retains its immunostimulatory activity during acetic acid fermentation.**

Vinegar can be made from various raw materials, such as grapes, apples, rice, and wheat, and is widely used as a flavoring agent and preservative. In Japan, vinegar is traditionally made from rice (1). The fermentation process used to produce rice vinegar involves the saccharification of rice by the Koji mold *Aspergillus oryzae*, alcohol fermentation by the Sake yeast *Saccharomyces cerevisiae*, and the oxidation of ethanol to acetic acid by acetic acid bacteria such as *Acetobacter pasteurianus*. Lactic acid bacteria are also observed during the early and late stages of fermentation.

Black unpolished rice vinegar, kurozu, is a common traditional Japanese vinegar with a characteristic dark amber color. The fermentation process used to produce it usually requires 2 years of fermentation and aging. Most of the organisms associated with fermentation die off during this process, and so microbial components are expected to be present in the vinegar. Previously, we found that the hydrophobic fraction of kurozu, which was obtained by hydrophobic interaction chromatography, stimulates induction of cytokine production (2). The immunostimulatory components in the fraction are expected to originate from the bacteria used in the fermentation process. We suspect that a lipoprotein and/or LPSs are responsible for the immunostimulatory effects of the fraction. The SDS-PAGE profile of the fraction displayed ladder patterns in the range from 15 to 75 kDa, and 3-hydroxy (3-OH)[2] fatty acids were found in it (2), suggesting that it contains LPS as a Toll-like receptor 4 (TLR4) agonist candidate. The immunostimulatory LPS appeared to be derived from *A. pasteurianus*, an aerobic Gram-negative rod; however, its structure could not be elucidated because the fraction was composed of a complex mixture, and the immunostimulatory component seemed to be resistant to weak acid hydrolysis.

LPSs are outer membrane components of Gram-negative bacteria and exhibit immunostimulatory and inflammatory effects (3). They are composed of a heterogeneous mixture of macromolecular amphiphilic compounds consisting of a polysaccharide part, a core oligosaccharide, and a glycolipid anchor

* This work was supported in part by the Adaptable and Seamless Technology Transfer Program through Grant AS2111291E from the Japan Science and Technology Agency and Grants-in-Aid for Scientific Research 23510259 and 26350961 from the Japan Society for the Promotion of Science. The authors declare that they have no conflicts of interest with the contents of this article.

[1] To whom correspondence should be addressed: Dept. of Chemistry, Biotechnology, and Chemical Engineering, Kagoshima University, Korimoto 1-21-40, Kagoshima 890-0065, Japan. Tel./Fax: 81-99-285-7742; E-mail: hassy@eng.kagoshima-u.ac.jp.

[2] The abbreviations used are: 3-OH, 3-hydroxy; Kdo, 3-deoxy-D-manno-oct-2-ulosonic acid; TLR, Toll-like receptor; GlcN, glucosamine; ABEE, 4-aminobenzoic acid ethyl ester; GlcA, glucuronic acid; GlcN3N, 2,3-diamino-2,3-dideoxyglucose; Ko, D-glycero-D-talo-oct-2-ulosonic acid; ESI, electrospray ionization; TOCSY, total correlation spectroscopy; NOESY, nuclear Overhauser effect spectroscopy; HSQC, heteronuclear single quantum coherence; KdoO, Kdo 3-hydroxylase; Ap-LPS, *A. pasteurianus* LPS; Ap-LA1, *A. pasteurianus* lipid A.

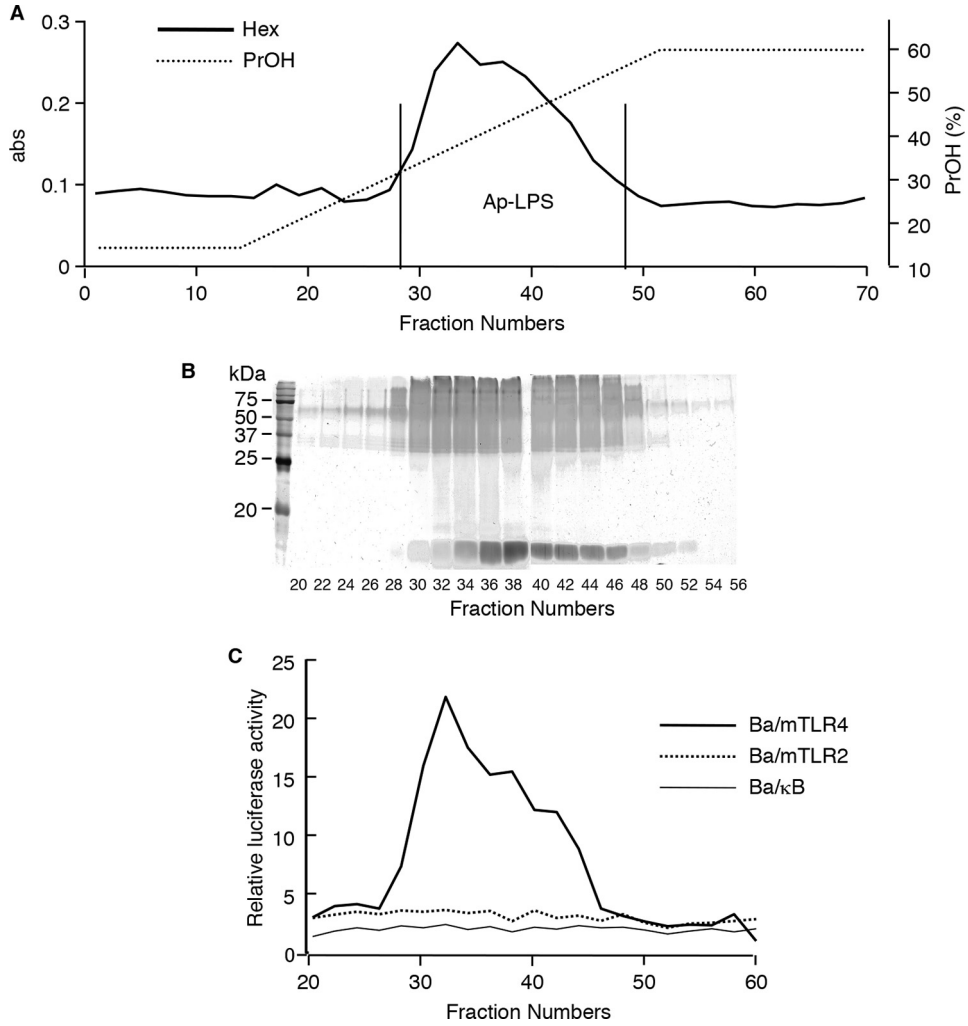

FIGURE 1. **Separation of LPS from *A. pasteurianus* bacteria.** *A*, elution profile of phenol-water extract according to hydrophobic interaction chromatography. The extract was subjected to an Octyl Sepharose 4FF column and eluted with a linear gradient of 1-propanol. The collected fractions had their hexose contents analyzed. *B*, the SDS-PAGE profiles of each fraction. The components of the fractions were separated in 15% gel and visualized by periodic acid-silver staining. *C*, the NF-κB activation induced by each fraction. The fractions were evaporated to remove the 1-propanol and dissolved in medium. Ba/κB, Ba/mTLR2, or Ba/mTLR4/mMD-2 cells were incubated with each test specimen for 4 h. NF-κB activation was measured with a luciferase assay.

called lipid A (4). The typical polysaccharide part consists of an O-antigen composed of a variable number of oligosaccharide repeating units. The structure of the polysaccharide section is extremely variable and is the main determining factor affecting the antigenicity of the LPS in the host. The core oligosaccharide region often contains L-glycero-D-manno-heptose, 3-deoxy-D-manno-oct-2-ulosonic acid (Kdo), and several sugars. The lipid A moiety is known to be essential for the immunostimulatory effects of LPS on the mammalian immune system and has been shown to stimulate the TLR4-MD-2 complex (5). The chemical structures of many types of lipid A have been characterized (6). For example, the classical lipid A from *Escherichia coli* consists of a glucosamine (GlcN) disaccharide backbone, β-GlcN(1–6)α-GlcN, together with phosphate groups at the O-1 of the reducing GlcN and the O-4′ of the non-reducing GlcN, and six fatty acids, including four 3-OH fatty acids and two saturated fatty acids, branching off from the backbone. The polysaccharide section is linked to the core region, and the core is connected to the lipid A moiety by a ketosidic linkage of its reducing end Kdo residue (7). In LPS, the ketosidic bond between the Kdo residue and the lipid A moiety is relatively acid-labile, and hence, the LPS can be cleaved into a hydrophilic polysaccharide and a small lipid A molecule by weak acid hydrolysis. However, the LPS in the hydrophobic fraction from kurozu retains its macromolecular structure in acidic conditions, at least during the 2-year fermentation process. Thus, we hypothesized that this stability is due to the structure of the LPS molecule. In this study, we isolated the LPS from *A. pasteurianus* and characterized the structure of its lipid A moiety and immunobiological properties.

Results

Isolation of A. pasteurianus LPS—An LPS preparation was obtained from *A. pasteurianus* NBRC 3283 bacterial cells by hot phenol-water extraction followed by hydrophobic interaction chromatography of the crude aqueous extract. The elution profile of the LPS preparation demonstrated a single hexose-containing peak in the propanol gradient region (Fig. 1*A*), and its SDS-PAGE profile displayed a ladder pattern after periodic acid oxidized silver staining, indicating that fractions 28–48

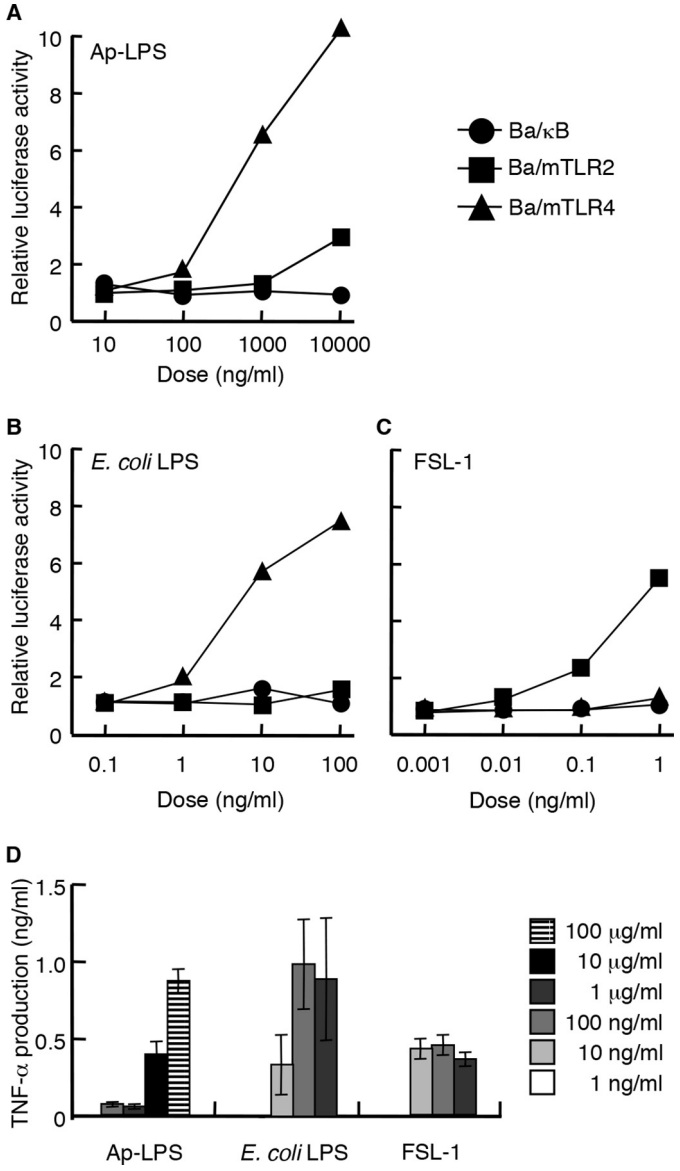

FIGURE 2. **Immunostimulatory activity of Ap-LPS.** *A–C*, the NF-κB activation induced in Ba/κB, Ba/mTLR2, or Ba/mTLR4/mMD-2 cells by Ap-LPS (*A*), *E. coli* LPS (*B*), or FSL-1 (*C*). The cells were incubated for 4 h, and the activity induced by each reagent was measured with a luciferase assay. *D*, TNF-α production induced by the indicated concentrations of each stimulus in murine spleen cells. The levels of TNF-α in the culture supernatants of the cells incubated for 4 h were measured by ELISA. *E. coli* LPS and FSL-1 were utilized as positive controls for TLR4 and TLR2, respectively.

contained LPS (Fig. 1*B*). The NF-κB activation assay showed that most of the above fractions stimulated TLR4 (Fig. 1*C*). Thus, fractions 28–48 were combined and designated as Ap-LPS. There were no LPS-like molecules in phenolic extract.

The immunostimulatory activity of Ap-LPS was investigated. Ap-LPS induced NF-κB activation in the Ba/mTLR4 cells (Fig. 2*A*). However, the NF-κB stimulatory activity of Ap-LPS was ~100-fold weaker than that of *E. coli* LPS (Fig. 2*B*). Ap-LPS also induced very slight NF-κB activation in the Ba/mTLR2 cells (Fig. 2*A*), probably because of Gram-negative bacterial lipoprotein contamination (8). In addition, Ap-LPS induced TNF-α production in murine spleen calls (Fig. 2*D*). However, this activity was also considerably weaker ($\sim 10^{-3}$) than that of *E. coli* LPS.

Isolation of A. pasteurianus Lipid A—The lipid A moiety is known to be responsible for the effects of LPS on the mammalian immune system. Therefore, Ap-LPS was subjected to weak acid hydrolysis to cleave the acid-labile Kdo bond and liberate the lipid A moiety. The hydrolysate was then partitioned using a solvent system composed of chloroform-methanol-water to obtain a hydrophobic fraction in the organic phase and a hydrophilic fraction in the aqueous phase. The TLC profile of the hydrophobic fraction demonstrated the existence of two main compounds (Fig. 3*A*). The ESI-TOF-MS spectrum of the fraction, which was obtained in negative ion mode, displayed two major doubly charged pseudomolecular ions $[M\text{-}2H]^{2-}$ at *m*/*z* 1083.2 and 1202.3 (Fig. 3*B*). The fatty acids in the hydrophobic fraction mainly consisted of 3-OH fatty acids, *i.e.* 14:0(3-OH) and 18:0(3-OH), and 16:0 fatty acids in the ratio 1.8:2.0:1.0. Because 3-OH fatty acids are only found in the lipid A moiety of the LPS molecule, these compounds were considered to be lipid A components. Thus, the fraction was separated by preparative TLC to obtain two compounds, which displayed higher (R_f 0.2, Ap-LA1) and lower (R_f 0.1, Ap-LA2) mobility (Fig. 3*A*). The ESI-TOF-MS spectrum of Ap-LA1 displayed a doubly charged ion at *m*/*z* 1202.3, and that of Ap-LA2 showed a doubly charged ion at *m*/*z* 1083.2. The mass difference between the ions was 238 units, which corresponded to a 16:0 fatty acid group. The ESI-TOF-MS spectrum of hydrazine-treated Ap-LA1, *i.e.* *O*-deacylated lipid A, displayed a doubly charged ion at *m*/*z* 850.8 (data not shown), indicating that Ap-LA1 contained two 16:0 fatty acids and one 14:0(3-OH) *O*-acylated fatty acid. These findings suggested that Ap-LA2 was an Ap-LA1 analogue that lacked a 16:0 fatty acid. Thus, the subsequent analyses were performed using Ap-LA1.

The immunostimulatory activity of *A. pasteurianus* lipid A was then investigated. Ap-LA1 induced NF-κB activation in Ba/mTLR4 cells (Fig. 4*A*); however, the activity of Ap-LA1 was ~100-fold weaker than that of *E. coli* lipid A molecule compound 506 (Fig. 4*B*). It did not induce NF-κB activation in Ba/mTLR2 cells (Fig. 4*A*), suggesting that lipid A moiety is not responsible for the TLR2 stimulating activity in AP-LPS. Ap-LA1 induced TNF-α production in murine spleen cells (Fig. 4*D*). This activity was also considerably weaker than that of compound 506.

In SDS-PAGE, the hydrophilic fraction after weak acid hydrolysis of Ap-LPS still displayed a ladder-like pattern (Fig. 3*C*). In addition, fatty acid analysis showed that the fraction contained 14:0(3-OH), 18:0(3-OH), and 16:0 fatty acids. These results indicated that the liberation of the lipid A moiety was incomplete. However, further weak acid hydrolysis did not alter the SDS-PAGE pattern of the hydrophilic fraction or liberate more lipid A. These results suggested that a proportion of the LPS molecules might use acid-stable D-glycero-D-talo-oct-2-ulopyranosylonic acid (Ko) to bind the polysaccharide section to the lipid A moiety.

Structure of A. pasteurianus Lipid A—Sugar compositional analysis of Ap-LA1 was performed with the 4-aminobenzoic acid ethyl ester (ABEE) labeling method. In this method, 2,3-diamino-2,3-dideoxyglucose (GlcN3N; 4.2 min), GlcN (6.7 min), and Man (13.2 min) were detected in HPLC profile using solvent A, and GlcA (5.6 min) and Man (10.2 min) were

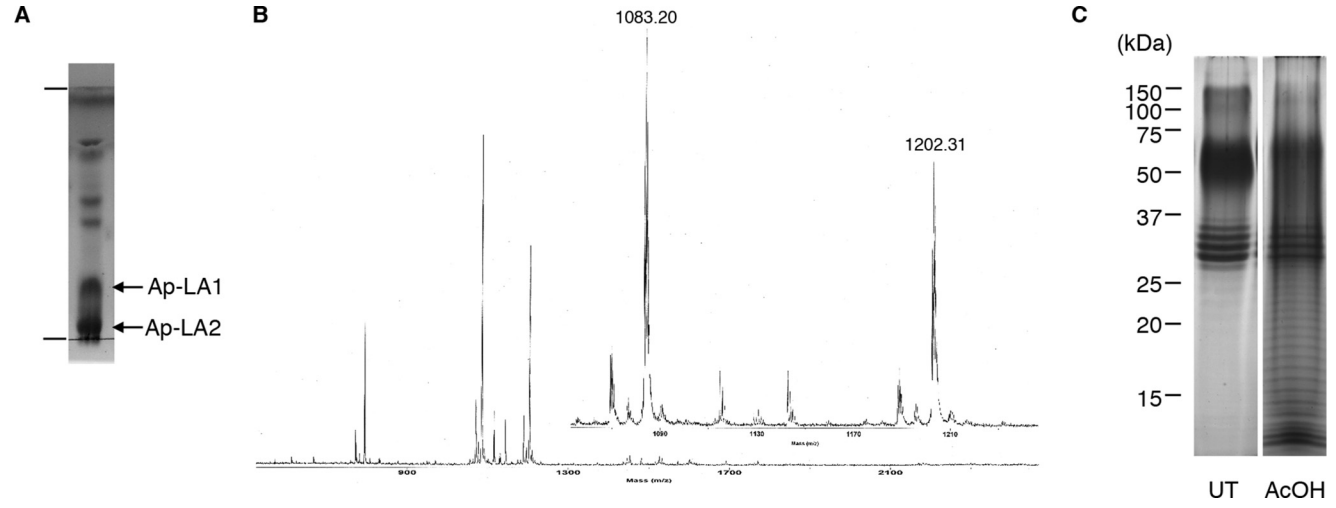

FIGURE 3. **Isolation of lipid A from *A. pasteurianus* LPS.** *A*, TLC profile of the hydrophobic fraction obtained by weak acid hydrolysis followed by phase partitioning. TLC was performed using a solvent system consisting of CH_3Cl-CH_3OH-H_2O (65/25/4, v/v/v) and visualized using anisaldehyde-sulfuric acid reagent. *B*, ESI-TOF-MS spectra of the hydrophobic fraction. The spectra were obtained with a Mariner instrument in negative ion refractor mode. *C*, SDS-PAGE profile of the untreated (*UT*) or hydrophilic fraction after weak acid hydrolysis (*AcOH*). The components were separated in 15% gel and visualized by periodic acid-silver staining.

observed in solvent B. The absolute configurations of the sugars were determined by the (*R*)-2-butyl glycoside method. The main peaks of the derivatives of GlcA, Man, and GlcN in Ap-LA1 were detected at 9.35, 9.93, and 11.57 min, respectively, and determined as D-configuration by comparison with commercially available standard sugars. That of GlcN3N in ApLA was found at 11.98 min, and the elution time was agreed with that of GlcN3N in lipid A from *Mesorhizobium loti* (9). However, the absolute configuration of GlcN3N could not be estimated because there is no available standard synthetic sugar.

The absolute configurations of the 3-OH fatty acids were determined by (*R*,*S*)- or (*S*)-phenylethylamide 3-methoxy derivatives. In the (*R*,*S*)-phenylethylamide derivatives of 3-OH fatty acids in Ap-LA, the peaks for 14:0(3-OH) were detected at 14.73 and 14.89 min, and those for 18:0(3-OH) were detected at 17.70 and 17.88 min, respectively. In the (*S*)-phenylethylamide derivatives, the peaks for 14:0(3-OH) and 18:0(3-OH) were found at 14.74 and 17.71 min, respectively. It was previously reported that the (*S*)-phenylethylamide derivative of (*R*)-3-OH fatty acid (designated as *R*-*S*) eluted faster than the (*S*-*S*)-derivative (10). Because (*S*-*S*)-derivative is enantiomer of (*R*-*R*)-derivative, (*S*-*R*)-derivative elutes faster than (*R*-*R*)-derivative. These results showed that 3-OH fatty acid determined as *R*-configuration.

The molecular mass of Ap-LA1 was predicted to be 2406.6 from ESI-MS analysis (Fig. 3*B*). In contrast, the molecular mass of estimated lipid A composed of found components, Man, GlcN3N, GlcN, GlcA, two 16:0, two 14:0 (3-OH), and two 18:0 (3-OH), was 2170.6. The mass difference between the observed (2406.6) and estimated (2170.6) was 236 units, suggesting that the isolated lipid A was composed of four sugars, six fatty acids, and an unidentified component(s), whose molecular mass is 236.

Thus, the structures of the lipid A backbone sugars were analyzed by NMR spectroscopy. Sections of their one-dimensional and two-dimensional NMR spectra are shown in Fig. 5. The ^1H and ^{13}C NMR spectra of lipid A were assigned using COSY, total correlation spectroscopy (TOCSY), NOESY, and heteronuclear single quantum coherence (HSQC), and the resultant data are summarized in Tables 1 and 2. Five sets of sugar signals (A, B, C, D, and E) were observed in the COSY and TOCSY spectra of Ap-LA1 (Fig. 5, *A* and *B*). In spin system A, the two carbons at A2 and A3 displayed signals at δ53–54 (Fig. 5*C*), indicating that sugar A had a 2,3-diaminohexose structure. These NMR data agreed with that of the 2,3-diacylated GlcN3N of lipid A (11). The low field shifts of the protons at A2 and A3 compared with free NH_2 (12) were indicative of *N*-acylation at these positions. A β-linkage was assigned to the anomeric proton at δ4.35 because of its relatively small $^1J_{C,H}$ value (166 Hz) and its relatively large $^3J_{H,H}$ value (8.1 Hz) (13, 14). Other $^3J_{H,H}$ values indicated the glucopyranosyl configuration. Thus, sugar A was determined to be β-GlcN3N. The characteristic singlet-like signal of H1 in spin system B was indicative of mannopyranosyl configuration. The relatively large $^1J_{C,H}$ value (175 Hz) of the anomeric position indicated that sugar B was α-Man. In spin system C, carbon C2 was shifted to δ51.2, which was indicative of GlcN structure. The low field shifts of the protons at C2 and C3 were suggestive of *N*,*O*-acylation at these positions. An α-linkage was assigned to the anomeric proton at δ5.06 because of its relatively large $^1J_{C,H}$ value (181 Hz) and its relatively small $^3J_{H,H}$ value (3.4 Hz). Other $^3J_{H,H}$ values indicated the glucopyranosyl configuration. Thus, sugar C was considered to be α-GlcN. One proton at C6 was not detected probably because it should be under fatty acids signals around δ3.94. Spin system D consisted of five protons and carbons, which was indicative of GlcA. The relatively large $^1J_{C,H}$ value (179 Hz) and relatively small $^3J_{H,H}$ value (3.6 Hz) of the anomeric proton suggested an α-linkage. Other $^3J_{H,H}$ values indicated the glucopyranosyl configuration. Thus, sugar D was determined to be α-GlcA. Spin system E consisted of seven protons but did not contain an anomeric proton. The relatively small coupling constants for $^3J_{3,4}$ and $^3J_{4,5}$ and the very small one for $^3J_{5,6}$ were indicative of a *talo* configuration. Furthermore, the ^{13}C NMR data of sugar E

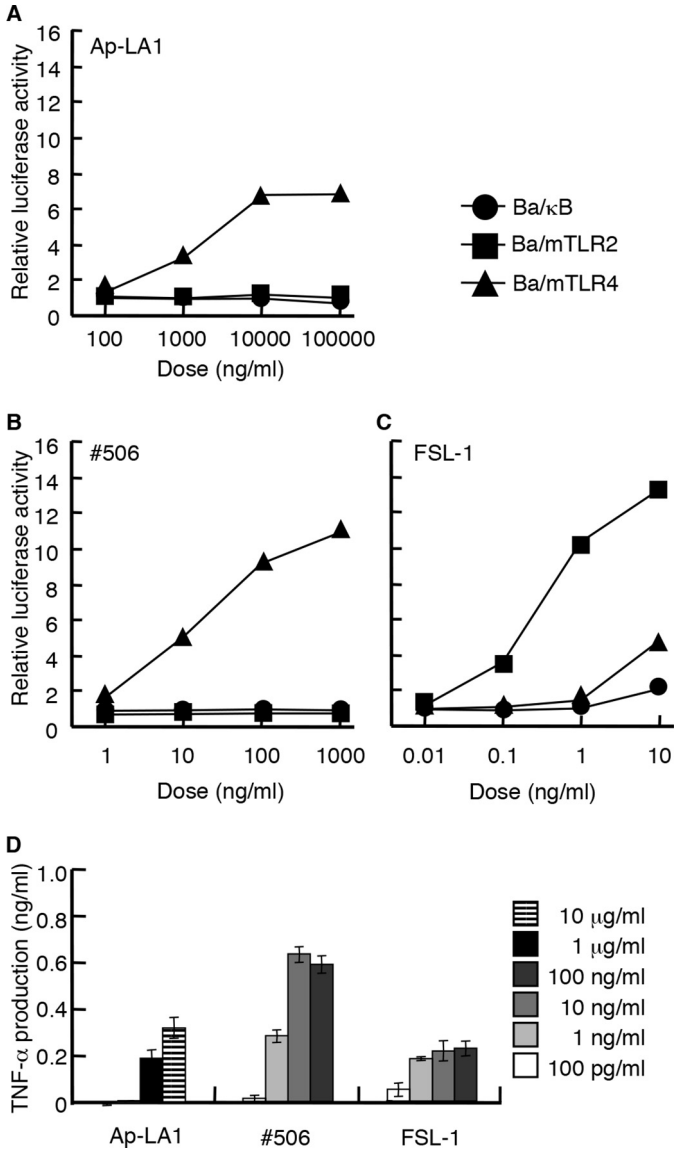

FIGURE 4. **Immunostimulatory activity of Ap-LA1.** *A–C*, the NF-κB activation induced in Ba/κB, Ba/mTLR2, or Ba/mTLR4/mMD-2 cells by Ap-LA1 (*A*), compound 506 (*B*), or FSL-1 (*C*). The cells were incubated for 4 h, and the level of activity induced by each reagent was measured with a luciferase assay. *D*, TNF-α production induced by the indicated concentration of each stimulus in murine spleen cells. The levels of TNF-α in the culture supernatants of the cells incubated for 4 h were measured by ELISA. Compound 506 and FSL-1 were utilized as positive controls for TLR4 and TLR2, respectively.

agreed with that of synthetic α-Ko derivatives (15). These findings indicated that sugar E was α-Ko. The molecular mass of dehydrated form of Ko was 236 units, suggesting that the unidentified component in Ap-LA1 was Ko. This finding agreed with the above observation that some of the LPS remained stable during weak acid hydrolysis.

The inter-residual NOESY coupling from proton B1 to A4 suggested that a glycosidic linkage exists between the α-Man (B) and 4 position of β-GlcN3N (A) (Fig. 5*D*). The downfield shift of the ^{13}C signal of A4 compared with 4-*O*-unsubstituted GlcN3N (9, 11) indicated that sugar A was a 4-*O*-substituted GlcN3N (Table 2). The inter-residual coupling from A1 to C6 revealed the presence of glycosylation between β-GlcN3N (A) and the 6 position of the α-GlcN residue (C) (Fig. 5*D*), and the downfield shift of the ^{13}C signal of C6 demonstrated that it was a 6-*O*-substituted GlcN (Table 2). The NOESY coupling from C1 to D1/D5 and from D1 to C1/C5 indicated the presence of a glycosidic link between position 1 of α-GlcN (C) and position 1 of α-GlcA (D) (Fig. 5*D*). Although no direct NOESY evidence for a link between the rest of the molecule and Ko (E) was observed, a slight (1.2 to 2.6 ppm) downfield shift was detected in the ^{13}C signal of A6 (9, 11, 16), suggesting a Ko(2–6)GlcN3N linkage. These results indicated that the *A. pasteurianus* lipid A molecule contains the following sugar backbone: α-Man(1–4)[α-Ko(2–6)]β-GlcN3N(1–6)α-GlcN(1–1)α-GlcA.

To determine the fatty acid distribution of the lipid A molecule, Ap-LA1 was analyzed with tandem MS (Fig. 6*A*). In the spectrum of the precursor ion at *m*/*z* 1202.3, several doubly and singly charged daughter ions were observed. The doubly charged ion at *m*/*z* 1110.4, which corresponded to the elimination of an aldehyde with the formula $C_{12}H_{24}O$ (calculated Δ184 units), arose from 14:0(3-OH) (16, 17). The singly charged ion at *m*/*z* 1985.7 resulted from the loss of Ko (Ko-18; calculated Δ236 units) from the doubly charged ion at *m*/*z* 1110.4. An ^{0,2}A-type fragment ion was detected at *m*/*z* 1888.6 (18). This fragment ion indicated that the *N*-acyl group at position 2 of GlcN was 18:0(3-OH), which was not further acylated. An ^{0,4}A-type fragment ion was also observed at *m*/*z* 1602.4, suggesting that the *O*-acyl group at position 3 of GlcN was a 14:0(3-OH) fatty acid. This coincided with the results of the de-*O*-acylation experiment described above. The doubly charged ions at *m*/*z* 1074.4 and 982.3 and the singly charged ions at *m*/*z* 1729.4, 1632.4, and 1346.1 were explained by the neutral loss of a 16:0 fatty acid (calculated Δ256 units) from the ions at *m*/*z* 1202.3, 1110.4, 1985.7, 1888.6, and 1602.4, respectively. These observations suggested that a 16:0 fatty acid was linked to position 3 of the 3-OH fatty acids. These results meant that the acyl groups attached to the GlcN3N residue were 14:0(3-O(16:0)) and 18:0(3-O(16:0)) fatty acids. However, their exact positions (C2 or C3) could not be determined. Taking these observations into account, the structure of *A. pasteurianus* NBRC 3283 lipid A was proposed to be as shown in Fig. 6*B*.

Discussion

Most Gram-negative bacteria possess LPS molecules. In the majority of LPS, the polysaccharide part is covalently attached to the lipid A moiety by a reducing end acid-labile Kdo residue (7). In this study, however, NMR spectroscopy detected Ko in the *A. pasteurianus* LPS. *A. pasteurianus* is used in the fermentation process used to produce vinegar (19) and is able to grow in acidic conditions. If *A. pasteurianus* possessed a Kdo-type LPS, then its LPS would be degraded during the abovementioned fermentation process as it takes place in acidic conditions. Therefore, the conversion of Kdo to Ko is considered to be necessary for bacterial survival in acidic conditions. Similarly, LPS from several bacteria, including *Acinetobacter*, *Burkholderia*, *Yersinia*, and *Serratia*, are known to utilize Ko instead of Kdo in their LPS (20). The biosynthetic pathway responsible for this has not been well defined. Recently, Kdo 3-hydroxylase (KdoO), which replaces the proton at the 3_{ax} position of Kdo with an OH group to give Ko, was found in several bacteria including *Burkholderia* and *Yersinia* (21). However, we could

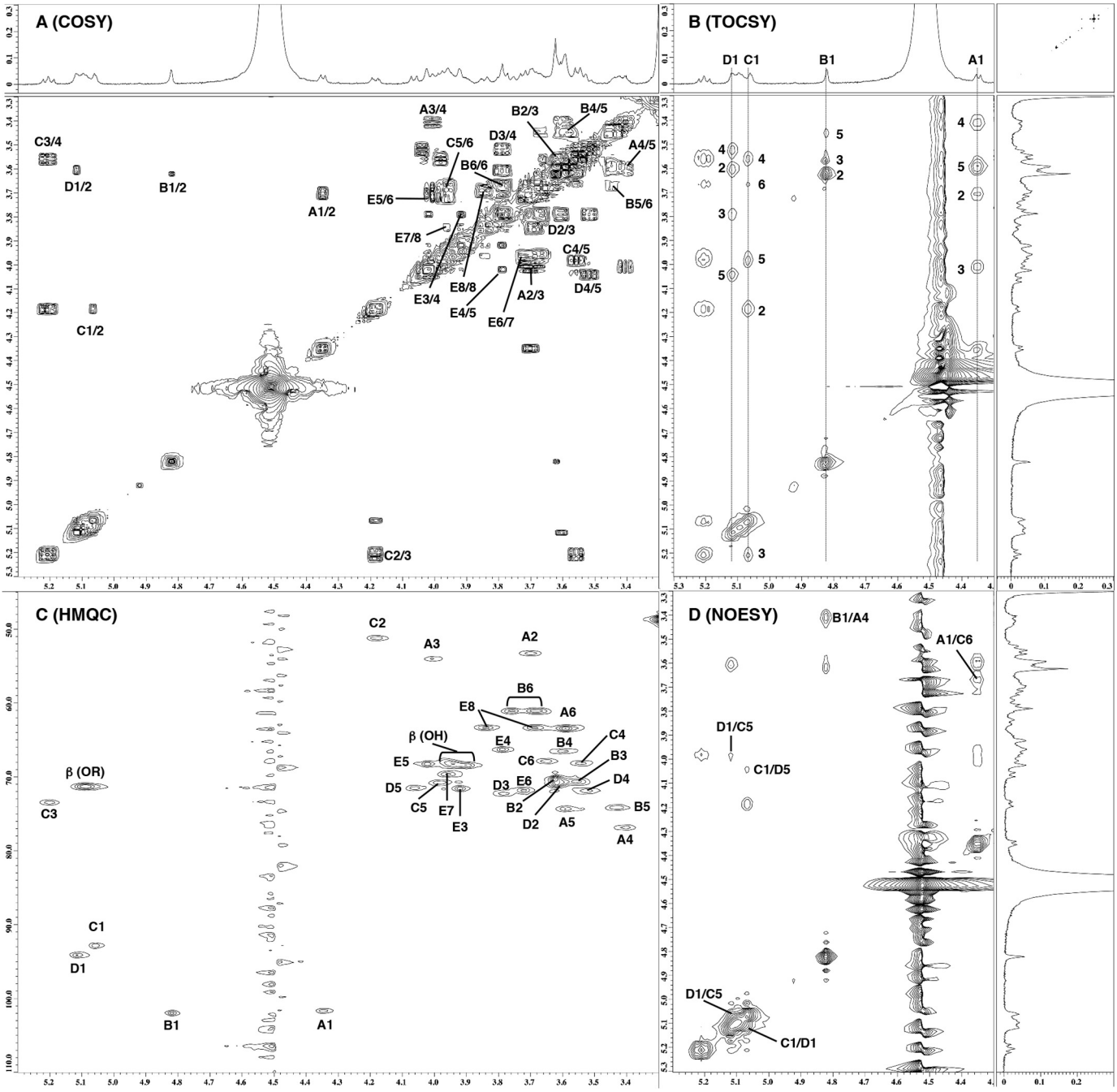

FIGURE 5. **Part of the two-dimensional ^{1}H NMR spectra of Ap-LA1.** *A*, COSY. *B*, TOCSY. *C*, HSQC. *D*, NOESY. The spectra were obtained at 293 K in $CDCl_3$–CD_3OD–D_2O (6/4/1, v/v/v).

TABLE 1

^{1}H NMR chemical shifts and coupling constants of the sugar backbone components of Ap-LA1

The spectra were recorded at 600 MHz in $CDCl_3$–CD_3OD–D_2O (6/4/1, v/v/v) at 293 K.

	Residues				
Position	α-Man (B)	β-GlcN3N (A)	α-GlcN (C)	α-GlcA (D)	Ko (E)
1	4.82 (~1)	4.35 (8.1)	5.06 (3.4)	5.12 (3.6)	
2	3.62 (5.6)	3.70 (10.8)	4.18 (10.8)	3.60 (9.7)	
3	3.56	4.01 (8.8)	5.21 (9.2)	3.79 (9.0)	3.92 (3.7)
4	3.59	3.40 (9.5)	3.56 (9.5)	3.52 10.0)	3.79 (3.8)
5	3.44	3.60	3.98	4.06	4.02 (~1)
6	3.67, 3.79	3.60	3.67		3.72 (8.8)
7					3.96 (3.1, 7.7)
8					3.69, 3.84 (11.1)

TABLE 2
^{13}C NMR chemical shifts and coupling constants of the sugar backbone components of Ap-LA1
The spectra were recorded at 151 MHz in $CDCl_3$–CD_3OD–D_2O (6/4/1, v/v/v) at 293 K. ND, not determined.

	Residues				
Position	α-Man (B)	β-GlcN3N (A)	α-GlcN (C)	α-GlcA (D)	Ko (E)
1	102.0 (175)	101.7 (166)	92.8 (181)	94.1 (179)	ND
2	70.4	53.3	51.2	70.9	ND
3	70.6	54.0	73.5	72.2	71.6
4	66.5	76.9	68.1	71.9	66.3
5	74.2	74.4	70.8	71.5	68.2
6	61.1	63.4	67.9	ND	71.8
7					69.6
8					63.3

not find a KdoO homologue in the *A. pasteurianus* NBRC 3283 genome (22) during a BLAST search. However, because the genomes of *Acinetobacter* species do not encode KdoO and other enzymes that perform the same function as KdoO have been suggested to exist (21), *A. pasteurianus* might synthesize Ko by another route.

We were able to obtain lipid A molecules containing a single Ko residue from *A. pasteurianus* LPS by weak acid hydrolysis. This is first study to isolate a Ko-substituted lipid A molecule. We could not obtain the Ko-containing lipid A direct extraction of untreated Ap-LPS, suggesting that the Ko-containing lipid A was not a deep rough LPS but a part of a smooth type LPS. In many bacteria, the core region contains a L-α-D-Hep^{II}-(1–3)-L-α-D-Hep^{I}-(1–5)-[α-Kdo^{II}-(2–4)]-α-Kdo^{I} tetrasaccharide, and Kdo^{I} forms a link with the lipid A moiety. In *Burkholderia*, *Yersinia*, and *Serratia*, only Kdo^{II} is replaced by Ko (20), and hence, these bacteria do not possess Ko-substituted lipid A molecules. Conversely, in *Acinetobacter* Kdo^{I} is replaced by Ko (Ko^{I}), which is directly linked to lipid A; however, Ko^{I} is substituted by Glc, which is used instead of Hep^{I} in the core oligosaccharide main chain in *Acinetobacter* (20). Thus, the Ko-substituted lipid A cannot be liberated by weak acid hydrolysis. However, Ko-GlcNol was isolated by strong acid hydrolysis (23). The fact that we were able to liberate Ko-substituted lipid A from *A. pasteurianus* LPS in the present study suggests that Kdo^{I} is replaced by Ko^{I} and an additional Kdo (Kdo^{a}) may be present in the core oligosaccharide main chain, which gives the following structure: core sugars-Kdo^{a}-Ko^{I}-lipid A. In addition, the existence of acid-resistant LPS (Fig. 3*C*) suggested that a certain proportion of the Kdo^{a} residues may be replaced by Ko. Conversely, we did not observe lipid A molecules without any Ko substitution, indicating that the conversion of Kdo^{I} to Ko^{I} was almost complete. A similar core structure was previously observed in *Acinetobacter baumannii* NCTC 10303 (24), although Kdo was not substituted for Ko in this molecule. Thus, the structure of the core region of *A. pasteurianus* NBRC 3283 LPS seems to be rare.

In addition, we detected a novel α-Man(1–4)β-GlcN3N(1–6)α-GlcN(1–1)α-GlcA sugar backbone structure in *A. pasteurianus* LPS (Fig. 6*B*). This structure is quite different from that of classical *E. coli* type lipid A (compound 506), *i.e.* the non-reducing end GlcN residue in the backbone disaccharide has been replaced with a GlcN3N residue, and the phosphate groups found at the *O*-1 position of the reducing end GlcN and the *O*-4′ position of the non-reducing end GlcN in compound 506 have been substituted for GlcA and Man residues, respectively. Because phosphate groups are relatively acid-labile, and trehalose-type glycosidic linkages are acid-stable, the above changes might represent adaptations to an acidic growth environment. Only a few atypical lipid A structures have been reported previously. GlcN3N(1–6)α-GlcN lipid A structures were found in *Flavobacterium* and *Arenibacter* (25, 26). In addition, a non-reducing end *O*-4′ Man substitution was detected in *Bradyrhizobium* (27), and a reducing end *O*-1 GlcA substitution was found in *Azorhizobium* (16). These bacteria are often found in soil or water. Although the biological roles of these atypical lipid A molecules are unknown, they might be required for survival in particular habitats.

Previously, Taniguchi *et al.* (28) reported that LPS from *Acetobacter aceti*, an acetic acid bacterium that is similar to *A. pasteurianus*, induced nitric oxide and TNF production in macrophages via TLR4. We also found that LPS/lipid A from *A. pasteurianus* stimulated TLR4 to induce NF-κB activation and cytokine release (Figs. 2 and 4). However, their effects were significantly weaker than those of *E. coli* LPS/lipid A. Because lipid A is essential for the immunostimulatory activity of LPS (4), the atypical structure of *A. pasteurianus* lipid A might be responsible for its weak activity. The structure-activity relationships of lipid A have been investigated using *E. coli* lipid A. The minimal requirement for potent cytokine-inducing activity is a compound 506-type structure, *i.e.* two gluco-configured hexosamine residues, two phosphate groups, and six fatty acids. Partially structurally deficient lipid A molecules are less active or inactive. In particular, the number of phosphate groups and the number and length of the fatty acyl groups significantly influence the activity of lipid A molecules. However, it should be mentioned that although atypical lipid A molecules were considered to exert weak biological activity because of the weak activities of the corresponding LPS (29, 30), the activity of isolated lipid A molecules has not been directly investigated. In this study, we demonstrated the biological activity of isolated *A. pasteurianus* lipid A (Fig. 4). As a result, we found that it displayed 100–1000-fold weaker activity than *E. coli* lipid A compound 506. This reduction in activity might have been mainly caused by the replacement of the non-reducing end phosphate group with a Man residue. Studies of synthetic carboxymethylated lipid A (31, 32) have suggested that the carboxylate group belonging to the reducing end GalA residue is responsible for the residual activity of *A. pasteurianus* lipid A. Conversely, the longer fatty acyl groups of *A. pasteurianus* lipid A might be responsible for its diminished activity.

In conclusion, we isolated the *A. pasteurianus* LPS molecule and elucidated the chemical structure of its lipid A moiety. As a result, we found that the *A. pasteurianus* lipid A molecule possesses a novel and quite atypical backbone structure that contains Man, GlcN3N, and GlcA and is connected to the core region of the LPS molecule via a Ko residue instead of a Kdo residue. In addition, it is considered to be more acid-stable than typical LPS. We also demonstrated that *A. pasteurianus* LPS/lipid A possessed moderate immunostimulatory activity in comparison with those of *E. coli*. because of its atypical structure.

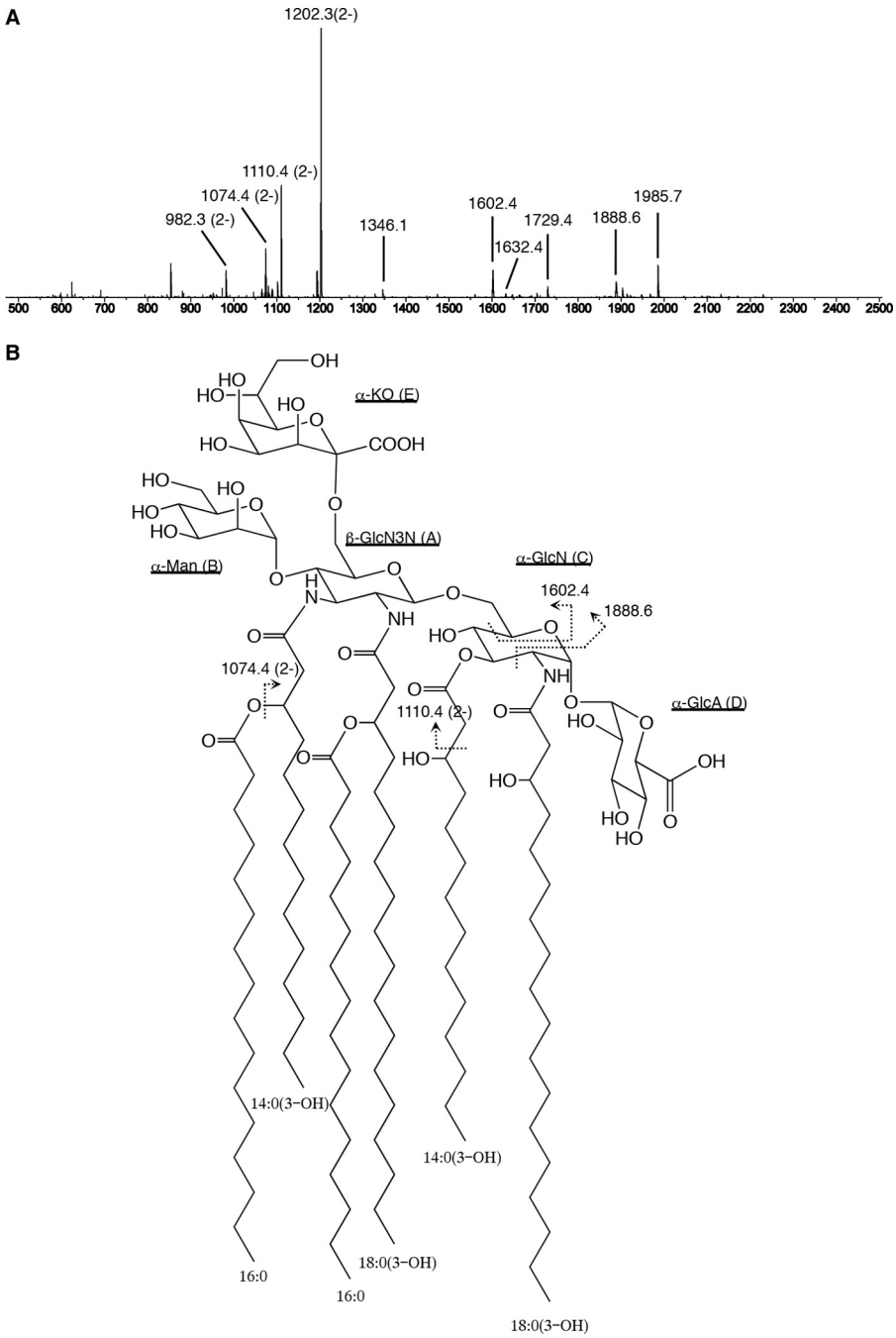

FIGURE 6. **Proposed structure of Ap-LA1.** *A*, tandem MS spectrum of the precursor ion at *m/z* 1202.3. The spectra were obtained with a Q-STAR XL instrument in negative and product ion scan modes. *B*, structure of Ap-LA1. The fatty acyl groups at positions 2 and 3 of GlcN3N are interchangeable. Proposed fragmentation points are indicated by *broken lines*.

Experimental Procedures

Bacterial Strain and Bacterial Components—A. pasteurianus NBRC 3283 was obtained from the National Institute of Technology and Evaluation Biological Resource Center (Chiba, Japan). The bacteria were cultured in No.804 broth, which consisted of 0.5% polypeptone, 0.5% yeast extract, 0.5% glucose, and 0.1% magnesium sulfate heptahydrate, at 37 °C for 2 days. The bacterial cells were harvested by centrifugation and then washed three times with saline. After being lyophilized, the cells were subjected to phenol-water extraction to obtain a crude extract in the aqueous phase (33). The crude extract was digested with DNase and RNase and then with proteinase K to obtain crude LPS. The digest was subjected to hydrophobic interaction chromatography on an Octyl Sepharose 4FF column using a method similar to that described previously (34) to obtain an LPS preparation.

FSL-1, a synthetic diacylated lipopeptide that acts as a TLR2 ligand, was purchased from EMC Microcollections (Tübingen, Germany). *E. coli* O111:B4 ultrapure LPS (InvivoGen, San Diego, CA) was used as a TLR4-specific ligand. The *E. coli*-type lipid A compound 506 was synthesized as described previously (35).

Isolation of Lipid A—The LPS preparation was hydrolyzed with 0.6% acetic acid at 105 °C for 2.5 h. The hydrolysate was then partitioned using a solvent system composed of chloroform-methanol-water (2/1/3, v/v/v) to yield a hydrophobic fraction in the organic phase and a hydrophilic fraction in the aqueous phase. The hydrophobic components were separated by Silica Gel 60 TLC as described below to obtain the lipid A fraction. De-*O*-acylation was performed by anhydrous hydrazine treatment according to the previously described method (36).

Analytical Methods—Hexose content was measured using the anthrone-sulfuric acid assay (37). Analytical SDS-PAGE was performed with the Tris-glycine method (38). The gels were visualized with Coomassie Brilliant Blue or periodic acid-silver staining (39).

Sugar composition was analyzed using the ABEE method (40). The target samples were hydrolyzed with 4 M TFA at 100 °C for 6 h and then labeled with ABEE using the standard method. The labeled sugars were analyzed with an LC-10 HPLC system (Shimadzu, Kyoto, Japan). Namely, the ABEE-labeled sugars were injected into a Honenpak C18 column (4.6 × 75 mm; J-oil mills, Tokyo, Japan), eluted with solvent A (0.02%TFA-acetonitrile; ratio: 90/10, v/v) or B (0.2 M potassium borate buffer, pH 8.9, acetonitrile; ratio: 93/7, v/v) at 45 °C at a flow rate of 1.0 ml/min, and then had their fluorescence detected (excitation: 305 nm, emission: 360 nm). Man, GlcN, and glucuronic acid GlcA were used as standard sugars. Standard GlcN3N was obtained from the hydrolysate of *M. loti* lipid A (9, 11).

The absolute configurations of the sugars were determined by the (*R*)-2-butyl glycoside method (41). The target samples were hydrolyzed with 4 M TFA at 100 °C for 6 h or 6 M HCl at 100 °C for 18 h and then *N*-acetylated with pyridine-acetic anhydride-methanol. The monosaccharides were labeled with (*R*)-2-butanol as described. The labeled sugars were analyzed with an GCMS-QP2010 system (Shimadzu) equipped with a DB-5 capillary column (0.25 mm × 30 m; Agilent, Santa Clara, CA). The temperature program was initially 150 °C for 1 min and then raised to 300 °C at a ramp rate of 10 °C/min; final time was 14 min.

Fatty acids were analyzed according to the methyl ester method (42). The target samples were methanolyzed with 5% hydrogen chloride-methanol at 100 °C for 3 or 18 h. The resultant fatty acid methyl esters were analyzed with a GC-2010 Plus (Shimadzu) equipped with a DB-1 capillary column (0.25 mm × 30 m; Agilent). The temperature program was initially 80 °C for 2 min and then raised to 290 °C at a ramp rate of 8 °C/min; final time was 15 min.

The absolute configurations of the 3-OH fatty acids were determined by (*S*)-phenylethylamide 3-methoxy derivatives (10). The above methanolyzed fatty acids were etherified with trimethylsilyldiazomethane, hydrolyzed the methyl ester, and then labeled with (*R*,*S*) or (*S*)-phenylethylamine using the described method. The phenylethylamide 3-methoxy derivatives were analyzed with the GC-MS system equipped with a DB-1 capillary column. The temperature program was initially 150 °C for 1 min and then raised to 325 °C at a ramp rate of 10 °C/min; final time was 14 min. Analytical and preparative TLC were performed on a TLC plate (No. 5715; Merck) using a solvent system consisting of chloroform-methanol-water (65/25/4, v/v/v), and the resultant spots were visualized with anisaldehyde-sulfuric acid reagent.

Luciferase and Cytokine Assay—Ba/F3 cells that stably expressed p55IgκLuc, an NF-κB/DNA binding activity-dependent luciferase reporter construct (Ba/κB), murine TLR2 and the p55IgκLuc reporter construct (Ba/mTLR2), or murine TLR4/MD-2 and the p55IgκLuc reporter construct (Ba/mTLR4) were kindly provided by Prof. K. Miyake (Institute of Medical Science, University of Tokyo, Tokyo, Japan). The NF-κB-dependent luciferase activity of these cells was determined as described previously (43). The results are shown as relative luciferase activity, which was determined as the ratio of stimulated to unstimulated activity.

Eight-week-old male BALB/c mice were obtained from Kyudo (Kumamoto, Japan). The animals received humane care in accordance with our institutional guidelines (approved as SE11002 at Kagoshima University) and the legal requirements of Japan. Mouse spleen cells were obtained from healthy BALB/c, suspended in RPMI1640 supplemented with 10% FBS, and distributed in 96-well plates at a density of 1×10^6 cells/well. The cells were stimulated with the indicated concentrations of the test specimens in culture medium at 37 °C for 4 h, and then the culture supernatants were collected. The cell supernatants were subjected to the cytokine assay using an ELISA kit for secreted TNF-α (R&D Systems, Minneapolis, MN). The concentrations of TNF-α secreted from the cells were determined using the standard curves for recombinant cytokines prepared in each assay. The results are shown as the means ± S.E. of the mean obtained from three independent experiments.

NMR Spectroscopy and Mass Spectroscopy (MS)—^{1}H and ^{13}C NMR spectra were measured at 600 and 151 MHz, respectively, on a JMN-ECA600 spectrometer (JEOL, Tokyo, Japan) equipped with an HX5 indirect detection gradient probe were obtained at 293K in $CDCl_3$–CD_3OD-D_2O (6/4/1, v/v/v). Chemical shifts are expressed in δ-values using CHD_2OD (δ 3.31) as an internal standard for the ^{1}H NMR spectra and CHD_2OD (δ 49.0) as an internal standard for the ^{13}C NMR spectra. The signals were assigned using COSY, TOCSY, NOESY, and HSQC spectroscopy. Coupling constants were determined by one-dimensional ^{1}H NMR in combination with J-resolved spectroscopy.

ESI-TOF-MS spectra were obtained using a Mariner instrument (AB SCIEX, Framingham, MA) in negative ion reflector mode. Tandem mass spectra were obtained in collision-induced dissociation mode using argon as the collision gas and a Q-STAR XL instrument equipped with a nanospray source (AB SCIEX) in the negative and product ion scan modes. The collision-induced dissociation parameter was −63 V for CE and 5 psi for CAD. The samples were dissolved in chloroform-methanol-water (6/4/1, v/v/v) and injected using a syringe pump or nanospray tip (Humanix, Hiroshima, Japan).

Author Contributions—M. H., S. H., Y. S., K. F., and Y. F. designed and developed the experiments. K. F. and Y. F. prepared standard compounds. M. H., M. O., M. F., and R. B. performed experiments. M. H. wrote and edited the manuscript.

Acknowledgments—We are grateful to Prof. Junichi Abe at Kagoshima University for support with the use of the Q-STAR XL instrument.

References

1. Murooka, Y., Nanda, K., and Yamashita, M. (2009) Rice vinegars. In *Vinegars of the World* (Solieri, L., and Giudici, P., eds) pp. 121–133, Springer-Verlag
2. Hashimoto, M., Obara, K., Ozono, M., Furuyashiki, M., Ikeda, T., Suda, Y., Fukase, K., Fujimoto, Y., and Shigehisa, H. (2013) Separation and characterization of the immunostimulatory components in unpolished rice black vinegar (kurozu). *J. Biosci. Bioeng.* **116,** 688–696
3. el-Samalouti, V. T., Hamann, L., Flad, H. D., and Ulmer, A. J. (2000) The biology of endotoxin. *Methods. Mol. Biol.* **145,** 287–309
4. Rietschel, E. T., Kirikae, T., Schade, F. U., Mamat, U., Schmidt, G., Loppnow, H., Ulmer, A. J., Zähringer, U., Seydel, U., and Di Padova, F. (1994) Bacterial endotoxin: molecular relationships of structure to activity and function. *FASEB J.* **8,** 217–225
5. Shimazu, R., Akashi, S., Ogata, H., Nagai, Y., Fukudome, K., Miyake, K., and Kimoto, M. (1999) MD-2, a molecule that confers lipopolysaccharide responsiveness on Toll-like receptor 4. *J. Exp. Med.* **189,** 1777–1782
6. Kabanov, D. S., and Prokhorenko, I. R. (2010) Structural analysis of lipopolysaccharides from Gram-negative bacteria. *Biochemistry* **75,** 383–404
7. Mayer, H., Tharanathan, R. N., and Weckesser, J. (1985) Analysis of lipopolysaccharides of Gram-negative bacteria. In *Methods in Microbiology* (Gottschalk, G., ed) pp. 157–207, Vol. 18, Academic Press, London, UK
8. Hashimoto, M., Asai, Y., and Ogawa, T. (2004) Separation and structural analysis of lipoprotein in a lipopolysaccharide preparation from *Porphyromonas gingivalis*. *Int. Immunol.* **16,** 1431–1437
9. Hashimoto, M., Tanishita, Y., Suda, Y., Murakami, E., Nagata, M., Kucho, K., Abe, M., and Uchiumi, T. (2012) Characterization of nitric oxide-inducing lipid A derived from *Mesorhizobium loti* lipopolysaccharide. *Microbes Environ.* **27,** 490–496
10. Gradowska, W., and Larsson, L. (1994) Determination of absolute configurations of 2-and 3-hydroxy fatty acids in organic dust by gas chromatography-mass spectrometry. *J. Microbiol. Methods* **20,** 55–67
11. Choma, A., and Sowinski, P. (2004) Characterization of *Mesorhizobium huakuii* lipid A containing both D-galacturonic acid and phosphate residues. *Eur. J. Biochem.* **271,** 1310–1322
12. Velasco, J., Moll, H., Knirel, Y. A., Sinnwell, V., Moriyón, I., and Zähringer, U. (1998) Structural studies on the lipopolysaccharide from a rough strain of *Ochrobactrum anthropi* containing a 2,3-diamino-2,3-dideoxy-D-glucose disaccharide lipid A backbone. *Carbohydr. Res.* **306,** 283–290
13. Altona, C., and Haasnoot, C. A. (1980) Prediction of anti and gauche vicinal proton-proton coupling constants in carbohydrates: A simple additivity rule for pyranose rings. *Org. Magn. Reson.* **13,** 417–429
14. Tvaroska, I., and Taravel, F. R. (1995) Carbon-proton coupling constants in the conformational analysis of sugar molecules. *Adv. Carbohydr. Chem. Biochem.* **51,** 15–61
15. Gass, J., Strobl, M., Loibner, A., Kosma, P., and Zähringer, U. (1993) Synthesis of allyl O-[sodium (α-D-glcero-D-talo-2-octulopyranosyl)onate]-(2–6)-2-acetamido-2-deoxy-β-D-glucopyranoside, a core constituent of the lipopolysaccharide from *Acinetobacter calcoaceticus* NCTC 10305. *Carbhydr. Res.* **244,** 69–84
16. Choma, A., Komaniecka, I., Turska-Szewczuk, A., Danikiewicz, W., and Spolnik, G. (2012) Structure of lipid A from a stem-nodulating bacterium *Azorhizobium caulinodans*. *Carbohydr. Res.* **352,** 126–136
17. Shaffer, S. A., Harvey, M. D., Goodlett, D. R., and Ernst, R. K. (2007) Structural heterogeneity and environmentally regulated remodeling of *Francisella tularensis* subspecies novicida lipid A characterized by tandem mass spectrometry. *J. Am. Soc. Mass Spectrom.* **18,** 1080–1092
18. Kussak, A., and Weintraub, A. (2002) Quadrupole ion-trap mass spectrometry to locate fatty acids on lipid A from Gram-negative bacteria. *Anal. Biochem.* **307,** 131–137
19. Nanda, K., Taniguchi, M., Ujike, S., Ishihara, N., Mori, H., Ono, H., and Murooka, Y. (2001) Characterization of acetic acid bacteria in traditional acetic acid fermentation of rice vinegar (komesu) and unpolished rice vinegar (kurosu) produced in Japan. *Appl. Environ. Microbiol.* **67,** 986–990
20. Holst, O. (2011) Structure of the lipopolysaccharide core region. In *Bacterial Lipopolysaccharides* (Knirel, Y. A., and Valvano, M. A., eds) pp. 21–39, Springer-Verlag
21. Chung, H. S., and Raetz, C. R. (2011) Dioxygenases in *Burkholderia ambifaria* and *Yersinia pestis* that hydroxylate the outer Kdo unit of lipopolysaccharide. *Proc. Natl. Acad. Sci. U.S.A.* **108,** 510–515
22. Azuma, Y., Hosoyama, A., Matsutani, M., Furuya, N., Horikawa, H., Harada, T., Hirakawa, H., Kuhara, S., Matsushita, K., Fujita, N., and Shirai, M. (2009) Whole-genome analyses reveal genetic instability of *Acetobacter pasteurianus*. *Nucleic Acids Res.* **37,** 5768–5783
23. Zähringer, U., Kawahara, K., and Kosma, P. (2013) Isolation and structural characterization of a (Kdo-isosteric) D- glycero-α-D-talo-oct-2-ulopyranosidonic acid (Ko) interlinking lipid A and core oligosaccharide in the lipopolysaccharide of *Acinetobacter calcoaceticus* NCTC 10305. *Carbohydr. Res.* **378,** 63–70
24. Vinogradov, E. V., Petersen, B. O., Thomas-Oates, J. E., Duus, J., Brade, H., and Holst, O. (1998) Characterization of a novel branched tetrasaccharide of 3-deoxy-D-manno-oct-2-ulopyranosonicacid: the structure of the carbohydrate backbone of the lipopolysaccharide from *Acinetobacter baumannii* strain NCTC 10303 (ATCC 17904). *J. Biol. Chem.* **273,** 28122–28131
25. Kato, H., Haishima, Y., Iida, T., Tanaka, A., and Tanamoto, K. (1998) Chemical structure of lipid A isolated from *Flavobacterium meningosepticum* lipopolysaccharide. *J. Bacteriol.* **180,** 3891–3899
26. Silipo, A., Molinaro, A., Nazarenko, E. L., Sturiale, L., Garozzo, D., Gorshkova, R. P., Nedashkovskaya, O. I., Lanzetta, R., and Parrilli, M. (2005) Structural characterization of the carbohydrate backbone of the lipooligosaccharide of the marine bacterium *Arenibacter certesii* strain KMM 3941(T). *Carbohydr. Res.* **340,** 2540–2549
27. Komaniecka, I., Choma, A., Lindner, B., and Holst, O. (2010) The structure of a novel neutral lipid A from the lipopolysaccharide of *Bradyrhizobium elkanii* containing three mannose units in the backbone. *Chemistry.* **16,** 2922–2929
28. Taniguchi, Y., Nishizawa, T., Kouhchi, C., Inagawa, H., Yamaguchi, T., Nagai, S., Tamura, A., and Soma, G. (2006) Identification and characterization of lipopolysaccharide in acetic acid bacteria. *Anticancer Res.* **26,** 3997–4002
29. Tsukushi, Y., Kido, N., Saeki, K., Sugiyama, T., Koide, N., Mori, I., Yoshida, T., and Yokochi, T. (2004) Characteristic biological activities of lipopolysaccharides from *Sinorhizobium* and *Mesorhizobium*. *J. Endotoxin Res.* **10,** 25–31
30. Komaniecka, I., Zdzisinska, B., Kandefer-Szerszen, M., and Choma, A. (2010) Low endotoxic activity of lipopolysaccharides isolated from *Bradyrhizobium*, *Mesorhizobium*, and *Azospirillum* strains. *Microbiol. Immunol.* **54,** 717–725
31. Seydel, U., Schromm, A. B., Brade, L., Gronow, S., Andrä, J., Müller, M., Koch, M. H., Fukase, K., Kataoka, M., Hashimoto, M., Kusumoto, S., and Brandenburg, K. (2005) Physicochemical characterization of carboxymethyl lipid A derivatives in relation to biological activity. *FEBS J.* **272,** 327–340
32. Fujimoto, Y., Adachi, Y., Akamatsu, M., Fukase, Y., Kataoka, M., Suda, Y., Fukase, K., and Kusumoto, S. (2005) Synthesis of lipid A and its analogues for investigation of the structural basis for their bioactivity. *J. Endotoxin Res.* **11,** 341–347
33. Westphal, O., and Jann, K. (1965) Bacterial lipopolysaccharides: extraction with phenol-water and further applications to the procedure. In *Methods in Carbohydrate Chemistry* (Whistler, R. L., ed) pp. 83–91, Vol. 5, Academic Press, New York
34. Fischer, W. (1990) Purification and fractionation of lipopolysaccharide from Gram-negative bacteria by hydrophobic interaction chromatography. *Eur. J. Biochem.* **194,** 655–661
35. Fukase, Y., Zhang, S.-Q., Iseki, K., Oikawa, M., Fukase, K., and Kusumoto, S. (2001) New efficient route for synthesis of lipid A by using affinity separation. *Synlett* **11,** 1693–1698

36. Haishima, Y., Holst, O., and Brade, H. (1992) Structural investigation on the lipopolysaccharide of *Escherichia coli* rough mutant F653 representing the R3 core type. *Eur. J. Biochem.* **203,** 127–134
37. Ashwell, G. (1957) Colorimetric analysis of sugars. *Methods Enzymol.* **3,** 73–105
38. Laemmli, U. K. (1970) Cleavage of structural proteins during the assembly of the head of bacteriophage T4. *Nature* **227,** 680–685
39. Tsai, C. M., and Frasch, C. E. (1982) A sensitive silver stain for detecting lipopolysaccharides in polyacrylamide gels. *Anal. Biochem.* **119,** 115–119
40. Yasuno, S., Kokubo, K., and Kamei, M. (1999) New method for determining the sugar composition of glycoproteins, glycolipids, and oligosaccharides by high-performance liquid chromatography. *Biosci. Biotechnol. Biochem.* **63,** 1353–1359
41. Gerwig, G. J., Kamerling, J. P., and Vliegenthart, J. F. (1978) Determination of the D and L configuration of neutral monosaccharides by high-resolution capillary GLC. *Carbohydr. Res.* **62,** 349–357
42. Ikemoto, S., Katoh, K., and Komagata, K. (1978) Cellular fatty acid composition in methanol utilizing bacteria. *J. Gen. Appl. Microbiol.* **24,** 41–49
43. Hashimoto, M., Tawaratsumida, K., Kariya, H., Aoyama, K., Tamura, T., and Suda, Y. (2006) Lipoprotein is a predominant Toll-like receptor 2 ligand in *Staphylococcus aureus* cell wall components. *Int. Immunol.* **18,** 355–362